View metadata, citation and similar papers at core.ac.uk
brought to you by CORE
provided by Jagiellonian Univeristy Repository

DOI: https://doi.org/10.5114/pjr.2019.91259

Received: 28.10.2019
Accepted: 04.11.2019
Published: 09.12.2019

POLISH JOURNAL of RADIOLOGY
http://www.polradiol.com

Original paper

Coronary computed tomography angiography using model-based iterative reconstruction algorithms in the detection of significant coronary stenosis: how the plaque type influences the diagnostic performance

Antonio Vizzuso[1A,D], Riccardo Righi[2B], Aldo Carnevale[2E,F], Michela Zerbini[2B], Giorgio Benea[2A], Melchiore Giganti[1A,E]

[1]University of Ferrara, Italy
[2]Arcispedale Sant'Anna of Ferrara, Italy

Abstract

Purpose: To evaluate the ability of coronary computed tomography angiography (CCTA) with model-based iterative reconstruction (MBIR) algorithm in detecting significant coronary artery stenosis compared with invasive coronary angiography (ICA).

Material and methods: We retrospectively identified 55 patients who underwent CCTA using the MBIR algorithm with evidence of at least one significant stenosis (≥ 50%) and an ICA within three months. Patients were stratified based on calcium score; stenoses were classified by type and by coronary segment involved. Dose-length-product was compared with the literature data obtained with previous reconstruction algorithms. Coronary artery stenosis was estimated on ICAs based on a qualitative method.

Results: CCTA data were confirmed by ICA in 89% of subjects, and in 73% and 94% of patients with CS < 400 and ≥ 400, respectively. ICA confirmed 81% of calcific stenoses, 91% of mixed, and 67% of soft plaques. Both the dose exposure of patients with prospective acquisition (34) and the exposure of the whole population were significantly lower than the standard of reference ($p < 0.001$ and $p = 0.007$).

Conclusions: CCTA with MBIR is valuable in detecting significant coronary artery stenosis with a solid reduction of radiation dose. Diagnostic performance was influenced by plaque composition, being lower compared with ICA for patients with lower CAC score and soft plaques; the visualisation of an intraluminal hypodensity could cause false positives, particularly in D1 and MO segments.

Key words: multidetector computed tomography, coronary artery disease, coronary CT angiography.

Introduction

In the last 20 years computed tomography (CT) has assumed a primary diagnostic role with an ever-expanding range of possibilities. The wide use of this method has brought about the need to reduce exposure to ionising radiation, in line with the principle underlying radiation protection, as expressed by the acronym ALARA (as low as reasonably achievable). Recent technological advances have focused on one of the factors influencing image quality; namely, the dose/noise ratio. It is in this context that reconstruction software takes on a major role. Indeed, thanks to more and more evolved algorithms and mathematical models, the noise, and therefore the dose, have been significantly reduced [1]. The evolution of these algorithms has seen the transition from the "filtered back

Correspondence address:
Dr. Aldo Carnevale, Department of Radiology, Arcispedale Sant'Anna of Ferrara, via A. Moro 8, 44124, Ferrara, Italy, e-mail: aldocarnevale@hotmail.it

Authors' contribution:
A Study design · **B** Data collection · **C** Statistical analysis · **D** Data interpretation · **E** Manuscript preparation · **F** Literature search · **G** Funds collection

This is an Open Access journal, all articles are distributed under the terms of the Creative Commons Attribution-Noncommercial-No Derivatives 4.0 International (CC BY-NC-ND 4.0). License (https://creativecommons.org/licenses/by-nc-nd/4.0/).

projection" (FBP) to the first hybrid iterative construction models (HIR) to reach the last step of this evolutionary scale as represented by the most recent model-based iterative reconstruction (MBIR) algorithms [2]. The last of these models critically reduces noise, increases the contrast resolution, and maintains densitometric homogeneity, allowing acquisitions at very low doses [3-9]. Increasing attention to dose exposure is further confirmed by the recent directive EURATOM 2013/59, which, for the first time in the European legislative framework of radioprotection, makes communication of the radiation dose to the patient compulsory.

Therefore, the increase in diagnostic investigations based on ionising radiation places great emphasis on evaluation and monitoring of the dose absorbed by each patient over time. A field of application of MBIR algorithms is cardiovascular imaging, in particular coronary CT angiography (CCTA) [10]. In recent years, several studies have investigated the effects of low-dose images acquired with the new MBIR techniques, comparing them with the HIR and the older FBP reconstructions, and no qualitative and quantitative differences were reported in terms of attenuation, noise, and image contrast/noise ratio [11-14]. Moreover, MBIR dose reduction systems have reduced patient exposure while maintaining high quality of the images [15-18]. Few studies, however, have evaluated how MBIR influences the quantitative estimate of coronary stenosis [1,19].

The aim of our study was to assess the diagnostic ability of CCTA compared to conventional invasive coronary angiography (ICA) in the detection of significant coronary stenosis (50% or greater) with MBIR.

Material and methods

The study was approved by the Institutional Review Board, and the requirement of informed consent to conduct this retrospective and observational study was waived.

We retrospectively identified all adult patients (aged > 18 years) who had performed a CCTA with evidence of at least one significant stenosis (≥ 50%) and an ICA within three months of CCTA, in the period from April 2016 to April 2018. The research was carried out through access to the radiological information system (PolaRIS, Carestream Health, Rochester, NY, USA) and the image archiving and transmission system PACS (Carestream PACS, Carestream Health, Rochester, NY, USA). Patients were enrolled as shown in Figure 1.

Fifty-five patients (42 males and 13 females with an average age of 64.4 ± 9.9 years and an average BMI of 27.7 kg/m^2) presented with our inclusion criteria. Patients were divided into two groups based on Agatston's calcium score (CS) (< 400 vs. ≥ 400), while all identified significant stenoses were classified by type (calcified, mixed, and soft). Notably, calcification was identified for density greater than 220 HU [20,21]; plaques with 50% or greater calcium were defined as calcified, and less than that as mixed [20,22]. Moreover, each stenosis was classified by the coronary segment involved, in accordance with the 16-segment coronary tree model of the AHA [23], with the addition of venous graft segments and arterial graft for patients with by-pass. The CCTAs were performed on a tomograph (Philips Brilliance iCT 256-Slice Scanner, Philips Healthcare, Amsterdam, The Netherlands), and images reconstructed with MBIR (Iterative Model Reconstruction IMR, Philips. Healthcare), using voltage based on BMI and automatic current modulation. Table 1 shows the main technical parameters of scanning; of particular interest are the average voltage of 100 Kv and the average current, which was 194.9 mAs for all patients, but which became 110.9 mAs when only the 34 patients who performed CCTAs with prospective acquisition were considered. The extent of each stenosis was calculated using data reconstruction software (IntelliSpace Portal 8.0, Philips Healthcare, Amsterdam, The Netherlands) as the area reduction on coronary axial images by two radiologists with more than 10 years of experience in cardiac imaging. If a coronary segment had more than one stenosis, only the most significant one was considered.

ICA angiograms were carried out in the cardiac angiography suite (Artis Zee Floor, Siemens, Erlangen, Germany) by three interventional cardiologists with more than 15 years of experience; all investigations were performed by trans-femoral arterial catheterisation, and a minimum of eight projections were obtained. From the angiographic images, the stenoses identified were

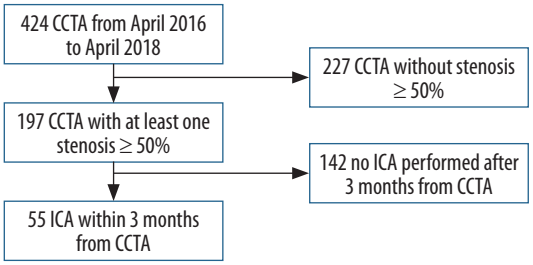

CCTA – coronary computed tomography angiography, ICA – invasive coronary angiography

Figure 1. Flow chart of the study population selection

Table 1. Scan parameters

CCTA with prospective scan mode	34
Beam collimation	256 × 0.625 mm
Slice thickness	0.9 mm
Reconstruction increment	0.3 mm
Rotation time	270 s
Tube voltage	100 kVp (80-120)
Tube current	194.9 mAs (70-539)
Tube current in prospective CCTA	110.9 mAs (70-273)
Field of view	18 cm

qualitatively evaluated, without specific quantitative or semi-quantitative software. The estimate of the vessel diameter reduction was, therefore, provided on the basis of the operator's experience.

The prevalence of CCTA diagnoses confirmed by ICA was calculated in the groups and subgroups defined by the collected variables (Figure 2).

The radiation dose measured in the sample was evaluated from the dose report of each CCTA using the dose-length product (DLP) and the effective dose (E_D). DLP was compared by means of the Wilcoxon signed-rank test with a review [18] evaluating the dose reduction associated with the HIR algorithms in the CCTAs. An alpha of 0.05 was used as the cut-off for significance, and the analyses were conducted on Stata 13 (StataCorp, 2013, College Station, TX).

Results

Of the 55 patients, 38 subjects had suspected acute coronary artery disease without prior cardiovascular events, while 17 patients had already undergone previous coronary interventions (six by-pass, nine angioplasties on native coronary, and two on venous grafts).

The number of stenoses identified on CCTA and ICA, in the groups and subgroups under examination, is reported in Table 2. CCTA stenoses confirmed by ICA were considered as CCTA true positives (TP), while the unconfirmed stenoses were false positives (FP).

The patient-based analysis showed that CCTA data were confirmed by ICA in 89% of subjects with at least one significant stenosis, and in 73% and 94% of patients with CS < 400 and ≥ 400, respectively. CS was not calculated in the 17 patients with previous revascularisation coronary interventions, so they were excluded. In the stenosis-based analysis, CCTA identified 129 stenoses and ICA confirmed 81% of them. ICA also confirmed 81% of calcified, 91% of mixed, and 67% of the soft stenoses (Figure 3).

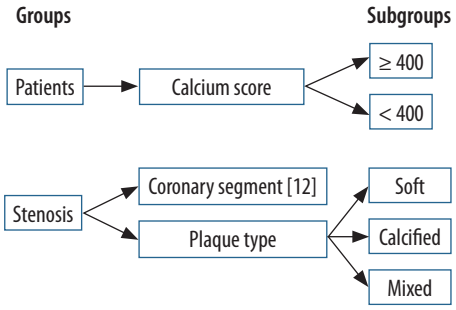

Figure 2. Graphic representation of the groups and subgroups for which the prevalence of confirmed diagnoses was to be calculated

Table 2. Group and subgroup populations; in the second column the number of patients with at least one significant stenosis and the number of significant stenoses identified by coronary computed tomography angiography (CCTA) and confirmed (TP) by invasive coronary angiography (ICA). In the third column the unconfirmed CCTA data (FP) by ICA

	CCTA ≥ 50%	ICA ≥ 50% (TP)	ICA < 50% (FP)
Patients	55	49	6
Patients with CS < 400	22	16	6
Patients with CS ≥ 400	16	15	1
Stenoses	129	105	24
Calcified stenoses	53	43	10
Mixed stenoses	46	42	4
Soft stenoses	30	20	10

Table 3 shows TP and FP stenosis and the correct diagnosis rate of CCTA based on the coronary segment stenosis.

The median DLP (mGy·cm) and E_D (mSv) were 187.4 and 2.6, respectively, in the entire population, but 125.4 and 1.8 when considering only the 34 patients with prospective acquisition. The Wilcoxon signed-rank test showed that both the dose exposure of patients with prospective acquisition and the exposure of the population as a whole were significantly lower than the DLP value of 240.8 ± 11.0 reported

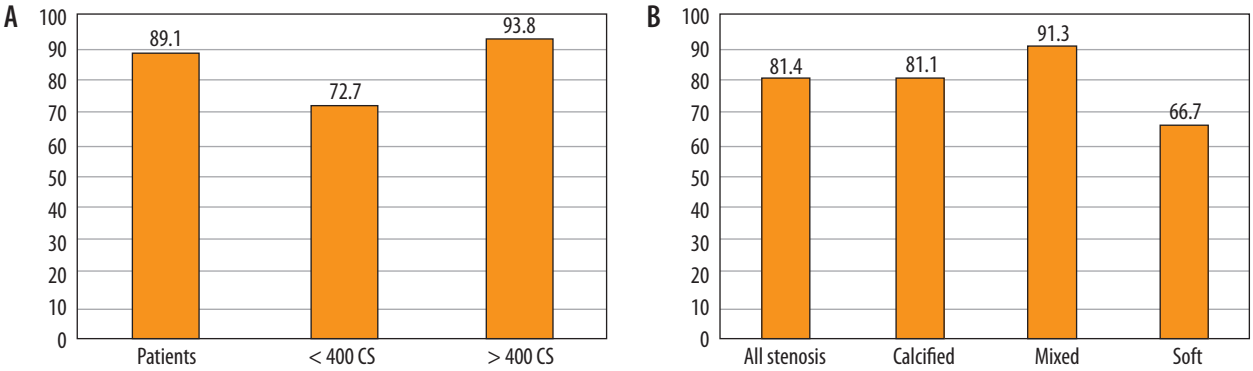

Figure 3. Histogram with percentage of coronary computed tomography angiography diagnoses confirmed by invasive coronary angiography. **A)** Patient-based analysis with at least one significant stenosis. **B)** Significant stenosis-based analysis

Table 3. Number of total stenoses divided per segment using the 16-segment coronary artery classification of the AHA with the arterial and venous graft segment addiction. The number of asterisks (*) indicates the number of intra-stent stenoses by segment

Coronary segments	TP	FP	%
Proximal RCA	8	3	72.7
Middle RCA	9	1	90.0
Distal RCA	5	1	83.3
rPDA	3	2	60.0
LMCA	4	1	80.0
Proximal LAD	26****	4	86.7
Middle LAD	13**	2	86.7
Distal LAD	3	1	75.0
D1	5	4	55.6
D2	0	0	0.0
Proximal CFx	12**	1	92.3
MO	3	4	42.9
Distal CFx	3	0	100.0
PL	1	0	100.0
IPDA	0	0	0.0
Ramus intermedius	4	0	100.0
Venous graft	3**	0	100.0
Arterial graft	3	0	100.0
Total number of stenoses	105	24	81.4

RCA – right coronary artery, rPDA – right postero-descending artery, LMCA – left main coronary artery, LAD – left anterior descendent artery, D – diagonal branch, Cfx – circumflex artery, MO – obtuse marginal branch, PL – postero-lateral branch, IPDA – left postero-descending artery

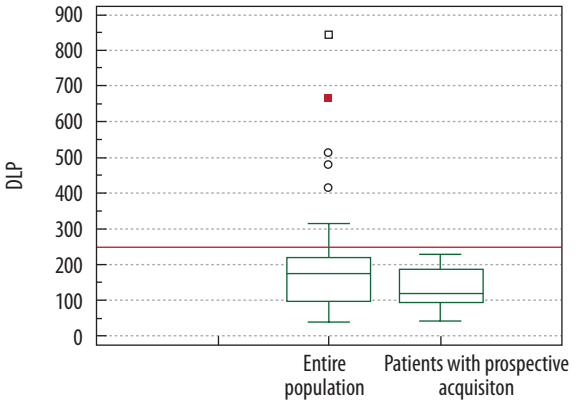

Figure 4. Box plot. Dose-length-product (DLP) distribution of the two populations (patients with prospective acquisition and the entire population) compared with our literature reference (red line)

in the literature (18), which was our standard of reference, with a $p < 0.001$ and $p = 0.007$, respectively (Figure 4).

Discussion

New technical advantages have significantly increased the ability to image the heart and coronary arteries, supporting the clinical utility of CCTA to analyse the coronary artery anatomy [24] and identify coronary artery stenosis [23]. Nowadays the main goal is to exclude coronary stenosis in subjects with low and intermediate pre-test probability of coronary disease, with atypical symptoms and/or unclear or inconclusive cardiologic investigations. Other indications are the follow-up of patients already treated with by-pass or coronary stents and in cases of suspected anomaly of coronary origin. CCTA is further indicated in candidate patients for cardiac surgery for valvular or aorta pathology [23,25-27]. The procedure has now been standardised [23,28].

Regarding the evaluation of coronary arteries, technological progress is proceeding along two parallel paths: on the one hand, the aim is to improve recognition of stenosis, quantify it correctly and, thanks to the estimate of the flow reserve [29], to evaluate its haemodynamic significance; on the other hand, research is oriented towards finding new strategies to reduce the dose, a goal that involves the previously mentioned iterative reconstructions. The final objective is a more widespread use of CCTA.

An important feature of CCTA is its high sensitivity (> 90%) and high negative predictive value (NPV > 98%) for the diagnosis of significant stenosis. The positive predictive value (PPV) reported in the main multicentre studies ranges from 64% to 86% to 91% [30-36]. These data support the main clinical indication of CCTA, which is to exclude the presence of significant stenosis in patients with pre-test probability of low or intermediate coronary disease.

Although the design of our study does not allow us to provide an evaluation of sensitivity, specificity, PPV, and NPV of CCTA in the detection of significant stenosis, it does provide us with the percentage of correct diagnoses of CCTA as compared with ICA, which we can, however, consider to be a substitute for the PPV. In accordance with data published in the literature [31-36], our results suggest that CCTA with MBIR may be considered reliable, showing a correct diagnosis rate of 89% for patients with at least one significant stenosis and 81% for total stenoses (Figures 5 and 6).

Furthermore, calcifications estimated by the calcium score (CS) represent a problem for the assessment of the vessel lumen. Calcium on the coronary wall tends to appear much larger than its real size (blooming effect). When the calcifications have high density and/or dimensions, they tend to obscure the vessel lumen [37], making assessment of the degree of stenosis difficult if not impossible. Recent data from the literature suggest that among the solutions to this problem, model-based iterative reconstruction techniques have been shown to improve image analysis for the morphological characterisation of coronary plaques, such as volume and composition, and consequently improve the evaluation of the degree of stenosis [38-40]. Our data seem to confirm this indication; in fact, we observed a higher percentage of correct diagnoses for patients with high coronary calcium burden (CS ≥ 400) and for calcified or mixed

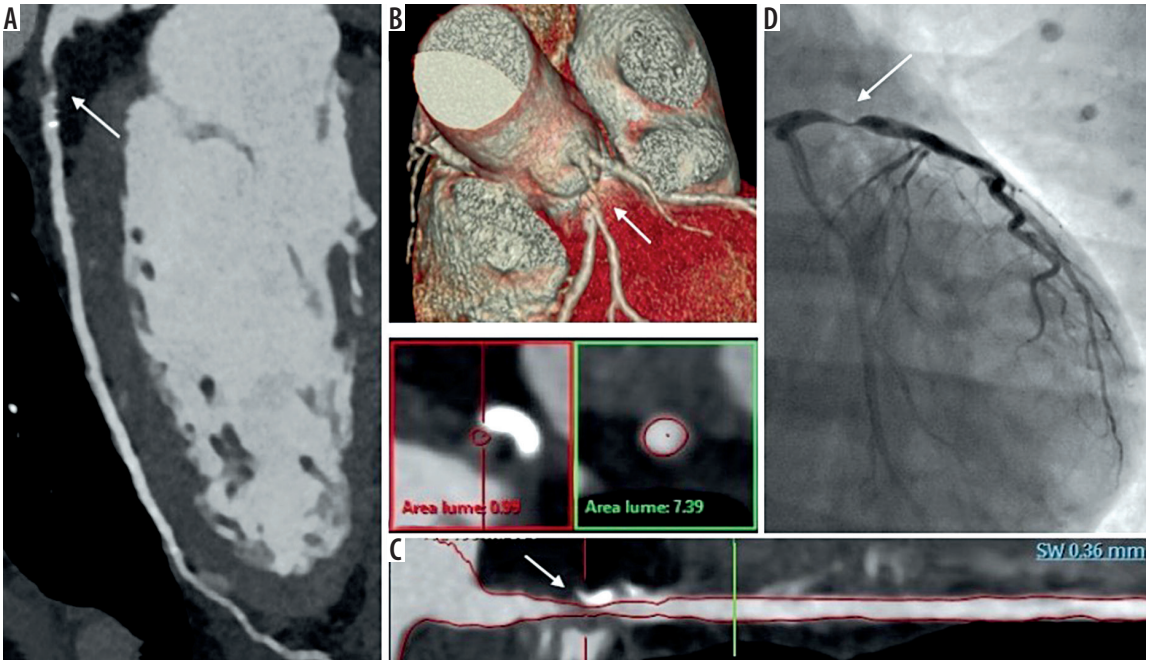

Figure 5. Coronary computed tomography angiography (CCTA) shows significant stenosis (arrows) in the proximal segment of left anterior descendent (LAD) branch confirmed by invasive coronary angiography (ICA). **A)** Curved multiplanar reformatted image of CCTA. **B)** CCTA 3-D volume rendering. **C)** True axial and longitudinal CT reconstruction of LAD at stenotic level. **D)** Fluoroscopic image during ICA

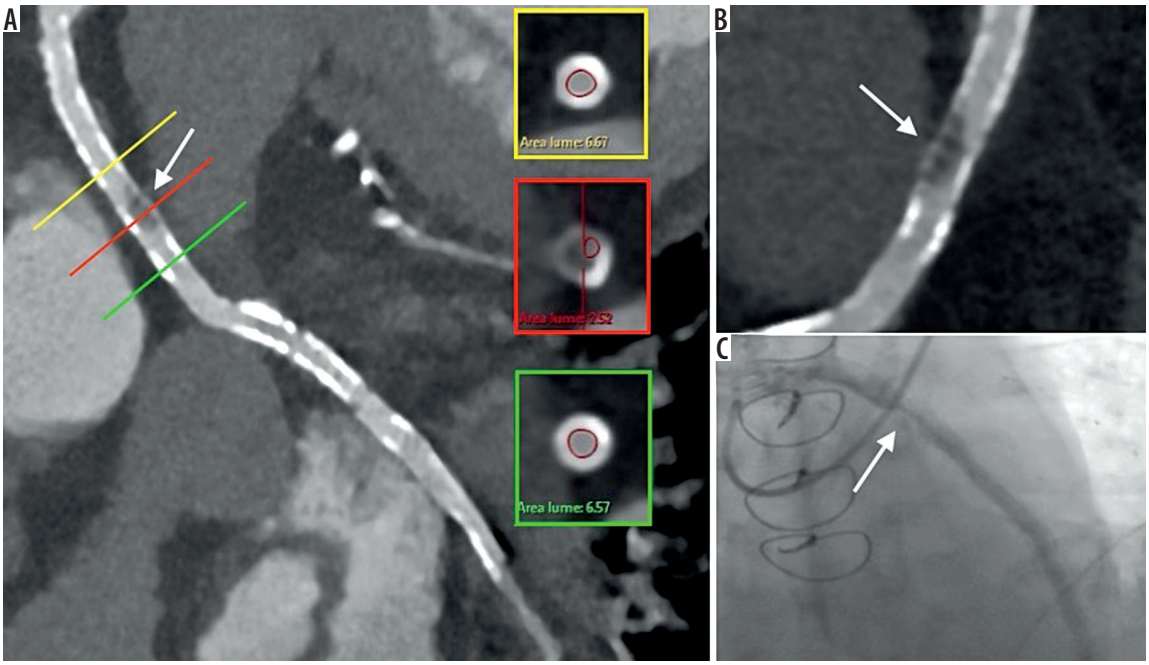

Figure 6. Patient with venous-graft by-pass. Coronary computed tomography angiography shows intra-stent hypodensity (arrows) in the venous graft confirmed by invasive coronary angiography (ICA). **A)** Curved multiplanar reformatted image with true axial sections of the vessel at stenotic level. **B)** Magnification of A. **C)** Fluoroscopic image during ICA

stenosis compared to the remaining subgroups. The use of MBIR algorithms for reducing blooming artefacts in the presence of coronary calcium has been demonstrated to reduce both the image noise and calcium scores compared to previous FBP [19,41].

Furthermore, in our experience, the presence of intraluminar hypodense bands of artefactual meaning, lacking in ICA evidence, and erroneously interpreted as significant plaques was connected to the low percentage (67%) of CCTA correct diagnoses of the soft plaques, which is an expression of a high number of FP. This artefact could be related to both the low dose and vessel geometry and/or turbulent flow in those coronary tracts, but further data are needed to better understand this phenomenon.

Broadly speaking, a diverse group of factors may affect the detection of non-calcified plaques in CCTA by radio-

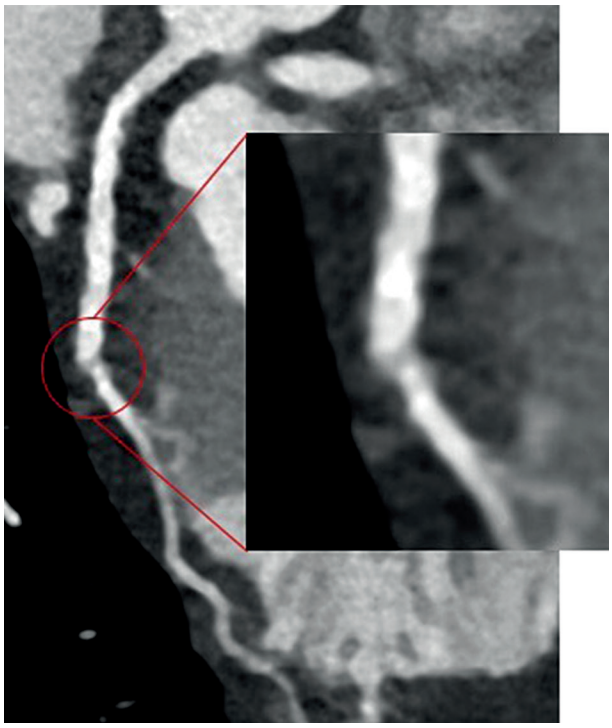

Figure 7. Curved multiplanar reformatted image of coronary computed tomography angiography shows D1 segment and magnification. At the origin of the branch, immediately after the emergence from left anterior descendent (LAD) branch, we can see the full thickness hypodense band misinterpreted as a significant stenosis (FP) and denied by the subsequent invasive coronary angiography

logists or even by computer-aided detection (CAD) systems [42], including the small calibre of coronary vessels, the image noise and limited spatial resolution of CT, and the intrinsic low contrast of the soft plaques. Nevertheless, most discrepancies between CCTA and ICA are probably due to the inferior temporal and spatial resolution of CCTA compared with ICA [43].

The 16-segment coronary tree model of the AHA [23] represents the basis for visual evaluation of significant coronary stenosis in segments with a lumen diameter ≥ 1.5 mm. The data in Table 3 show that the segments most affected by significant stenosis are proximal and middle left anterior descendent (LAD) branch with 87% of correct diagnoses, the right coronary artery (RCA) with 73% for proximal tract, 90% for middle tract, and 83% for distal tract, and proximal segment of Circumflex branch (CFx) with 92%. The number of stenoses on the other coronary segments, on the graft, and intra-stent is too small to make an evaluation in this setting. However, it should be noted that in the first diagonal (D1) and marginal obtuse (MO) segments, the high number of FP allows us to point out a low percentage of correct diagnoses: 56% and 46%, respectively. The retrospective analysis of CT images shows that the interpretation error mainly involves the proximal tract of these segments, which present a low attenuation band misinterpreted as stenosis (Figure 7).

The retrospective design of the study allows us to identify eight significant stenoses in the ICA but not recognised by CCTA, which we can consider as CT false negatives (FN). These were one stenosis on distal LAD segment, one on D1, one on second diagonal (D2) segment, one on acute marginal branch, one on distal RCA segment, two on posterolateral (PL) segment, and one on MO segment. These findings are of epidemiological interest but have no statistical value that goes beyond the aim of the study. We only stress that these FNs are mainly affected by distal segments and with a lumen diameter of < 1.5 mm.

In many studies, ICA remains the established gold standard for the diagnosis of coronary disease [30]. However, in some cases, ICA is not a good choice for the risk of non-negligible complications, such as arrhythmia, myocardial infarction, stroke, and access site problems. The examination also exposes the patient to greater amounts of ionising radiation. The issue concerning the radiation dose during CCTA is relevant in light of the potential stochastic cancer risk associated with radiation exposure for medical purposes. The literature tells us that the E_D for a standard ICA test is on average > 10 mS while for CCTA it is constantly < 10 mS and with the most recent technologies even < 1 mS [44,45]. Finally, we underline that almost a third of ICAs report findings of normal coronary artery [46,47].

In our experience, the MBIR reconstruction algorithm has been shown to reduce the radiation dose delivered to the patient, especially when combined with other dose reduction strategies, such as prospective acquisition.

ED was estimated by multiplying DLP with the conversion coefficient (ED/DLP) of 0.014 mSv/mGy · cm. ED/DLP value of 0.026 or 0.028 mSv/mGy · cm is actually the most accurate for the radiation dose estimate associated with cardiac CT compared to that used for chest CT scan (0.014 or 0.017 mSv/mGy · cm). However, the latter conversion factor is commonly used in many studies of cardiac CT. This discrepancy could lead to errors in comparing the E_D between different studies and so we used only DLP to compare the radiological exposure in our population with what is reported in the literature [18,25].

Our study has some limitations, such as its retrospective design with a limited population. Furthermore, we did not evaluate and stratify patients according to clinical symptoms, clinical pre-test probability of coronary disease, risk factors, or previous cardiovascular events because our exclusive interest was to evaluate the diagnostic capacity of IMR regardless of the type of patient performing the CCTA. We compared CCTA and ICA, but both methods have different approaches to estimate the extent of the stenosis, the latter using visual estimation of the vessel diameter reduction. Physician visual assessment of stenosis severity is the standard clinical practice to support decisions for coronary revascularisation; moreover, it has been demonstrated to be more accurate in predicting physiology than quantitative coronary angiography [48].

To make the methods more comparable, we decided to consider only the most significant stenosis per segment, even if a segment had more than one. We also analysed only the patients who were positive at CT, so we cannot express an opinion concerning sensitivity, specificity, PPV, and NPV of the method.

Conclusions

CCTA with MBIR has shown promising results for the detection of significant coronary stenosis with a solid dose reduction above all in the prospective acquisition modality. Performance is influenced by plaque composition, being lower in the case of patients with CS < 400 and soft plaques. The visualisation of an intraluminal hypodensity could cause false positive results, as in D1 and MO segments.

Disclosure

The authors declare no conflicts of interest.

References

1. Benz DC, Fuchs TA, Gräni C, et al. Head-To-head comparison of adaptive statistical and model-based iterative reconstruction algorithms for submillisievert coronary CT angiography. Eur Heart J Cardiovasc Imaging 2018; 19: 193-198.
2. Halliburton SS, Tanabe Y, Partovi S, et al. The role of advanced reconstruction algorithms in cardiac CT. Cardiovasc Diagn Ther 2017; 7: 527-538.
3. Fuchs TA, Stehli J, Bull S, et al. Coronary computed tomography angiography with model-based iterative reconstruction using a radiation exposure similar to chest X-ray examination. Eur Heart J 2014; 35: 1131-1136.
4. Kim H, Park CM, Song YS, et al. Influence of radiation dose and iterative reconstruction algorithms for measurement accuracy and reproducibility of pulmonary nodule volumetry: a phantom study. Eur J Radiol 2014; 83: 848-857.
5. Khawaja RDA, Singh S, Blake M, et al. Ultra-low dose abdominal MDCT: using a knowledge-based Iterative Model Reconstruction technique for substantial dose reduction in a prospective clinical study. Eur J Radiol 2015; 84: 2-10.
6. Park SB, Kim YS, Lee JB, et al. Knowledge-based iterative model reconstruction (IMR) algorithm in ultralow-dose CT for evaluation of urolithiasis: evaluation of radiation dose reduction, image quality, and diagnostic performance. Abdom Imaging 2015; 40: 3137-3146.
7. Lee ES, Kim SH, Im JP, et al. Effect of different reconstruction algorithms on computer-aided diagnosis (CAD) performance in ultra-low dose CT colonography. Eur J Radiol 2015; 84: 547-554.
8. Mehta D, Thompson R, Morton T, et al. Iterative model reconstruction: simultaneously lowered computed tomography radiation dose and improved image quality. Med Phys Int 2013; 1: 147-155.
9. Padole A, Ali Khawaja RD, Kalra MK, et al. CT radiation dose and iterative reconstruction techniques. Am J Roentgenol 2015; 204: W384-W392.
10. Naoum C, Blanke P, Leipsic J. Iterative reconstruction in cardiac CT. J Cardiovasc Comput Tomogr 2015; 9: 255-263.
11. Ippolito D, Riva L, Talei Franzesi CR, et al. Diagnostic efficacy of model-based iterative reconstruction algorithm in an assessment of coronary artery in comparison with standard hybrid-Iterative reconstruction algorithm: dose reduction and image quality. Radiol Med 2019; 124: 350-359.
12. Wang R, Schoepf UJ, Wu R, et al. Diagnostic accuracy of coronary ct angiography: comparison of filtered back projection and iterative reconstruction with different strengths. J Comput Assist Tomogr 2014; 38: 179-184.
13. Yin WH, Lu B, Li N, et al. Iterative reconstruction to preserve image quality and diagnostic accuracy at reduced radiation dose in coronary CT angiography: an intraindividual comparison. JACC Cardiovasc Imaging 2013; 6: 1239-1249.
14. Moscariello A, Takx RAP, Schoepf UJ, et al. Coronary CT angiography: image quality, diagnostic accuracy, and potential for radiation dose reduction using a novel iterative image reconstruction technique-comparison with traditional filtered back projection. Eur Radiol 2011; 21: 2130-2138.
15. Cha MJ, Seo JS, Yoo DS, et al. Knowledge-based iterative model reconstruction in coronary computed tomography angiography: comparison with hybrid iterative reconstruction and filtered back projection. Acta Radiol 2018; 59: 280-286.
16. Iyama Y, Nakaura T, Kidoh M, et al. Submillisievert radiation dose coronary CT angiography. Acad Radiol 2016; 23: 1393-1401.
17. André F, Fortner P, Vembar M, et al. Improved image quality with simultaneously reduced radiation exposure: Knowledge-based iterative model reconstruction algorithms for coronary CT angiography in a clinical setting. J Cardiovasc Comput Tomogr 2017; 11: 213-220.
18. Abdullah KA, McEntee MF, Reed W, et al. Radiation dose and diagnostic image quality associated with iterative reconstruction in coronary CT angiography: a systematic review. J Med Imaging Radiat Oncol 2016; 60: 459-468.
19. Lee J, Kim TH, Lee BK, et al. Diagnostic accuracy of low-radiation coronary computed tomography angiography with low tube voltage and knowledge-based model reconstruction. Sci Rep 2019; 9: 1308.
20. Saremi F, Achenbach S. Coronary plaque characterization using CT. AJR Am J Roentgenol 2015; 204: W249-W260.
21. Ozaki Y, Okumura M, Ismail TF, et al. Coronary CT angiographic characteristics of culprit lesions in acute coronary syndromes not related to plaque rupture as defined by optical coherence tomography and angioscopy. Eur Heart J 2011; 32: 2814-2823.
22. Dalager MG, Bøttcher M, Thygesen J, et al. Different plaque composition and progression in patients with stable and unstable coronary syndromes evaluated by cardiac CT. Biomed Res Int 2015; 2015: 401357.
23. Abbara S, Blanke P, Maroules CD, et al. SCCT guidelines for the performance and acquisition of coronary computed tomographic angiography: a report of the Society of Cardiovascular Computed

Tomography Guidelines Committee. J Cardiovasc Comput Tomogr 2016; 10: 435-449.
24. Vizzuso A, Righi R, Zerbini M, et al. An unusual presentation of anomalous left coronary artery from the pulmonary artery (ALCAPA) syndrome in a 70-year-old man: a case report. J Med Case Rep 2018; 12: 308.
25. Task Force Members, Montalescot G, Sechtem U, Achenbach S, et al. 2013 ESC guidelines on the management of stable coronary artery disease: the Task Force on the management of stable coronary artery disease of the European Society of Cardiology. Eur Heart J 2013; 34: 2949-3003.
26. di Cesare E, Carbone I, Carriero A, et al. Clinical indications for cardiac computed tomography. From the Working Group of the Cardiac Radiology Section of the Italian Society of Medical Radiology (SIRM). Radiol Med 2012; 117: 901-938.
27. Taylor AJ, Cerqueira M, Hodgson JM, et al.; American College of Cardiology Foundation Appropriate Use Criteria Task Force; Society of Cardiovascular Computed Tomography; American College of Radiology; American Heart Association; American Society of Echocardiography; American Society of Nuclear Cardiology; North American Society for Cardiovascular Imaging; Society for Cardiovascular Angiography and Interventions; Society for Cardiovascular Magnetic Resonance. ACCF/SCCT/ACR/AHA/ASE/ASNC/NASCI/SCAI/SCMR 2010 Appropriate Use Criteria for Cardiac Computed Tomography. A Report of the American College of Cardiology Foundation Appropriate Use Criteria Task Force, the Society of Cardiovascular Computed Tomography, the American College of Radiology, the American Heart Association, the American Society of Echocardiography, the American Society of Nuclear Cardiology, the North American Society for Cardiovascular Imaging, the Society for Cardiovascular Angiography and Interventions, and the Society for Cardiovascular Magnetic Resonance. J Cardiovasc Comput Tomogr 2010; 4: 407.e1-e33.
28. The American College of Radiology. ACR-NASCI-SPR practice parameter for the performance and interpretation of cardiac computed tomography (CT). 2016.
29. Nakansihi R, Budoff M. Noninvasive FFR derived from coronary CT angiography in the management of coronary artery disease: technology and clinical update. Vasc Health Risk Manag 2016; 12: 269-278.
30. Song Y Bin, Arbab-Zadeh A, Matheson MB, et al. Contemporary discrepancies of stenosis assessment by computed tomography and invasive coronary angiography. Circ Cardiovasc Imaging 2019; 12: e007720.
31. Budoff MJ, Dowe D, Jollis JG, et al. Diagnostic performance of 64-multidetector row coronary computed tomographic angiography for evaluation of coronary artery stenosis in individuals without known coronary artery disease. J Am Coll Cardiol 2008; 52: 1724-1732.
32. Miller JM, Rochitte CE, Dewey M, et al. Diagnostic performance of coronary angiography by 64-row CT. N Engl J Med 2008; 359: 2324-2336.
33. Meijboom WB, Meijs MFL, Schuijf JD, et al. Diagnostic accuracy of 64-slice computed tomography coronary angiography. J Am Coll Cardiol 2008; 52: 2135-2144.
34. SCOT-HEART investigators. CT coronary angiography in patients with suspected angina due to coronary heart disease (SCOT-HEART): an open-label, parallel-group, multicentre trial. Lancet 2015; 385: 2383-2391.
35. Munnur RK, Cameron JD, Ko BS, et al. Cardiac CT: atherosclerosis to acute coronary syndrome. Cardiovasc Diagn Ther 2014; 4: 430-448.
36. Sajjadieh A, Hekmatnia A, Keivani M, et al. Diagnostic performance of 64-row coronary CT angiography in detecting significant stenosis as compared with conventional invasive coronary angiography. ARYA Atheroscler 2013; 9: 157-163.
37. Kalisz K, Buethe J, Saboo SS, et al. Artifacts at cardiac CT: physics and solutions. Radiographics 2016; 36: 2064-2083.
38. Sun Z, Xu L. Coronary CT angiography in the quantitative assessment of coronary plaques. Biomed Res Int 2014; 2014: 346380.
39. Puchner SB, Ferencik M, Maehara A, et al. Iterative image reconstruction improves the accuracy of automated plaque burden assessment in coronary CT angiography: a comparison with intravascular ultrasound. Am J Roentgenol 2017; 208: 777-784.
40. Károlyi M, Szilveszter B, Kolossváry M, et al. Iterative model reconstruction reduces calcified plaque volume in coronary CT angiography. Eur J Radiol 2017; 87: 83-89.
41. Szilveszter B, Elzomor H, Károlyi M, et al. The effect of iterative model reconstruction on coronary artery calcium quantification. Int J Cardiovasc Imaging 2016; 32: 153-160.
42. Wei J, Zhou C, Chan HP, et al. Computerized detection of noncalcified plaques in coronary CT angiography: evaluation of topological soft gradient prescreening method and luminal analysis. Med Phys 2014; 41: 081901.
43. Kim J, Kwag HJ, Yoo SM, et al. Discrepancies between coronary CT angiography and invasive coronary angiography with focus on culprit lesions which cause future cardiac events. Eur Radiol 2018; 28: 1356-1364.
44. Sabarudin A, Sun Z. Radiation dose measurements in coronary CT angiography. World J Cardiol 2013; 5: 459-464.
45. Sun Z, Ng KH. Multislice CT angiography in cardiac imaging. Part III: radiation risk and dose reduction. Singapore Med J 2010; 51: 374-380.
46. Vijayalakshmi K, Kelly D, Chapple CL, et al. Cardiac catheterisation: radiation doses and lifetime risk of malignancy. Heart 2007; 93: 370-371.
47. Gerber TC, Carr JJ, Arai AE, et al. Ionizing radiation in cardiac imaging. Circulation 2009; 119: 1056-1065.
48. Adjedj J, Xaplanteris P, Toth G, et al. Visual and quantitative assessment of coronary stenoses at angiography versus fractional flow reserve. Circ Cardiovasc Imaging 2017; doi: 10.1161/CIRCIMAGING.117.006243.